

Reversible ordering and disordering of the vortex lattice in UPt₃

K. E. Avers,^{1,2} S. J. Kuhn,^{3,*} A. W. D. Leishman,³ W. J. Gannon,^{1,†} L. DeBeer-Schmitt,⁴ C. D. Dewhurst,⁵ D. Honecker,⁵ R. Cubitt,⁵ W. P. Halperin,¹ and M. R. Eskildsen^{3,‡}

¹*Department of Physics and Astronomy, Northwestern University, Evanston, Illinois 60208, USA*

²*Center for Applied Physics & Superconducting Technologies, Northwestern University, Evanston, Illinois 60208, USA*

³*Department of Physics, University of Notre Dame, Notre Dame, Indiana 46556, USA*

⁴*Large Scale Structures Section, Neutron Sciences Directorate,*

Oak Ridge National Laboratory, Oak Ridge, Tennessee 37831, USA

⁵*Institut Laue-Langevin, 71 avenue des Martyrs, CS 20156, F-38042 Grenoble cedex 9, France*

(Dated: March 1, 2025)

When studied by small-angle neutron scattering the vortex lattice (VL) in UPt₃ undergoes a gradual disordering as a function of time due to ²³⁵U fission. This temporarily heats regions of the sample above the critical temperature, where, upon re-cooling, the vortices remain in a quenched vortex glass state. The disordering rate is proportional to the magnetic field, suggesting that it is governed by collective VL properties such as the elastic moduli. An ordered VL can be re-formed by applying a small field oscillation, showing that the fission does not cause significant radiation damage to the UPt₃ crystals, even after long exposure.

Quantized vortices are introduced in a type-II superconductor subjected to an applied magnetic field [1]. Understanding and controlling vortex matter is of both fundamental interest and practical importance since vortex motion leads to dissipation. In an idealized scenario, vortices will arrange themselves in a perfectly ordered vortex lattice (VL) due to their mutual repulsion [2–4]. In reality, however, thermal effects and/or pinning to material defects is always present, and the balance between these competing factors determines the structural and dynamic properties of vortex matter [5–10]. This leads to a complex, high-dimensional phase diagram, where transitions between different states are driven not only by changes in intensive quantities, such as the field or temperature, but also the amount of imperfection or impurities which affect the vortex pinning. An example of the latter is columnar defects introduced by heavy ion irradiation [11]. In many applications control of vortex dynamics is of critical importance such as for high coherence in superconducting RF cavities used in accelerators [12] and potentially for quantum information science [13].

The ability to manipulate the vortices experimentally is essential to the study of vortex matter. Frequently, the VL configuration will depend on the field and temperature history, either in the degree of ordering [14–16] or the orientation of the VL relative to the crystalline axes of the host material [17–19]. In materials with weak vortex pinning, it is possible to anneal quenched disorder or dislodge the system from a ordered but metastable configuration by temporarily exciting the VL, either by applying a transport current [20–24] or a small-amplitude magnetic field oscillation [25–27]. This causes vortex motion and “shakes” them free of local minima in their collective energy landscape. In contrast, vortex matter in superconductors with strong pinning often become more disordered by the application of a vortex shaking [28–30].

Here we demonstrate a novel approach to structural

studies of vortex matter whereby reversible quenched disorder can be introduced locally without permanently affecting the host superconducting material. Specifically, we used small-angle neutron scattering (SANS) to study the VL in the topological superconductor UPt₃, which undergoes a gradual disordering on a time scale of tens of minutes as it is subjected to a beam of cold neutrons. The disordering is due to local heating events caused by neutron induced fission of ²³⁵U, which leaves an increasing fraction of the sample in a vortex glass state. While the system does not spontaneously re-order once the local heating has been dissipated, it is possible to re-anneal the VL by the application of a damped field oscillation.

The SANS measurements [31] were performed on the CG-2 General Purpose SANS instrument at the High Flux Isotope Reactor at Oak Ridge National Laboratory (ORNL) [32] and on the D33 instrument at the Institut Laue-Langevin (ILL) [33–35]. Two high-quality single crystals were studied, designated ZR8 and ZR11, with ZR8 being used in previous SANS measurements [36, 37]. The characteristics for each crystal is given in the Supplemental Material. Unless otherwise stated, SANS measurements were carried out in a “rocked on” configuration, satisfying the Bragg condition for VL peaks at the top of the two-dimensional position sensitive detector, as seen in Fig. 1. Measurements were performed at base temperature $\sim 50 - 65$ mK of a dilution refrigerator and with applied magnetic fields between 0.3 T and 1.0 T applied along the crystalline **c** axis. Background measurements, obtained either in zero field or above the upper critical field, were subtracted from the foreground data.

Prior to each SANS measurement sequence a pristine VL was prepared by applying a damped magnetic field oscillation with an initial amplitude of 20 mT around the measurement field. This was previously found to produce a well ordered VL with a homogeneous vortex density [37]. In addition, a ± 5 mT oscillation was applied periodically during some of the

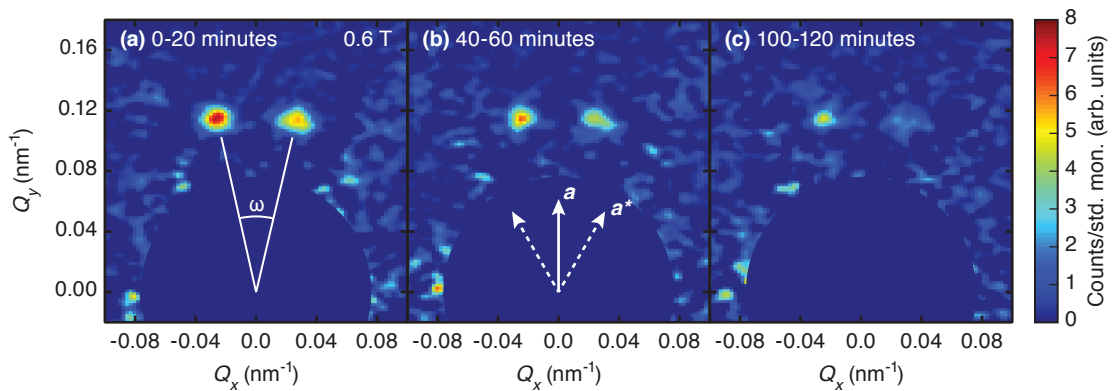


FIG. 1. Diffraction patterns obtained on ZR11 at 0.6 T (ORNL), measured at different times following the preparation of a pristine VL. Each was counted for 20 minutes and uses the same color scale. The peak splitting is indicated in (a) and crystallographic directions within the scattering plane in (b). Only peaks at the top of the detector were imaged. Background scattering is subtracted, and the detector center near $Q = 0$ is masked off.

SANS measurements to maintain an ordered VL [37]. All field oscillations end with a reduction of the magnetic field magnitude, corresponding to a decrease of the vortex density.

Figure 1 shows SANS VL diffraction patterns obtained illustrating the main result of this report. In all instances a pair of Bragg peaks are observed, split by an angle ω around the crystalline **a** axis as indicated in Fig. 1(a). A total of six such pairs exist, but to conserve beam time only the peaks at the top of the detector were brought into the Bragg condition. The split peaks correspond to VL domains rotated about the crystalline **c** axis in a clockwise or counter clockwise direction, with the intensity difference being due to an unequal domain population [37]. All diffraction patterns in Fig. 1 were recorded at the same temperature and magnetic field, and show a clear reduction of the intensity as a function of time. This reflects a gradual VL disordering and a corresponding broadening of the Bragg peaks in reciprocal space. Although the poor resolution within the detector plane makes the broadening difficult to resolve [31], it is clearly seen in the VL rocking curves discussed later. Note that what is characterized as an ordered VL is most likely a Bragg glass phase with algebraically decaying correlations [7, 8, 38–42], although it is not possible to establish this conclusively from the present SANS data.

To verify that the VL disordering is due to the neutron beam, measurements were performed both during a continuous exposure and following a prolonged period with the beam turned off. These are summarized in Fig. 2. Prior to the measurements a pristine VL was prepared, and the first data point (0-20 minutes) was collected while a ± 5 mT field oscillation was performed roughly every 60 seconds to maintain an ordered VL. The neutron shutter was then closed and the periodic field oscillation was turned off. After 90 minutes the shutter was re-opened and four subsequent 15 minute measurements of the VL intensity were made. The shutter was then closed again and a ± 5 mT field oscillation was applied to re-anneal the

VL. After an additional two hours, the shutter was opened for a final 15 minute measurement.

The data in Fig. 2 establish conclusively that the VL disordering occurs when the sample is illuminated by the neutron beam, and is attributed to ^{235}U fission events in the sample. Specifically, the intensity decreases to roughly half its initial value between 110 and 170 minutes, while no reduction is observed during the two periods where the beam was off. Figure 2 also confirms that an ordered VL is achieved by the application of the damped field oscillation, indicated by the recovery of the intensity both in the second and in the final data point. Finally, the intensity measured after the shutter opening at 110 and 290 minutes is somewhat higher than for the first data point. This is ascribed to the prolonged absence of fission heating of the UPt₃ crystals resulting in a lower overall sample temperature (see Supplemental Material). The possibility of a spontaneous re-ordering of the VL was also investigated. After one hour without beam exposure the intensity of a disordered VL was found to increase only modestly, with a count rate within measurement error of that recorded immediately before the beam

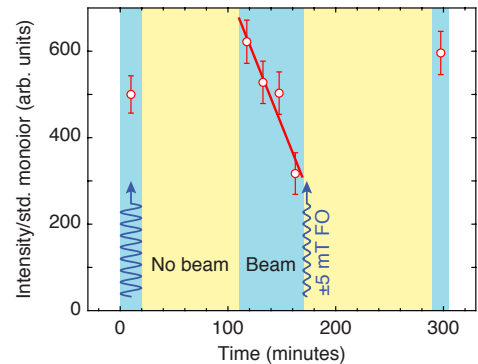


FIG. 2. Exposure test on ZR11 at 0.8 T (ORNL), where dark (light) shading indicate when the neutron beam was on (off). The VL scattered intensity is normalized to the standard monitor count. Field oscillations (FO) of ± 5 mT were applied periodically during the first measurement and at 170 minutes after the neutron beam was shut off.

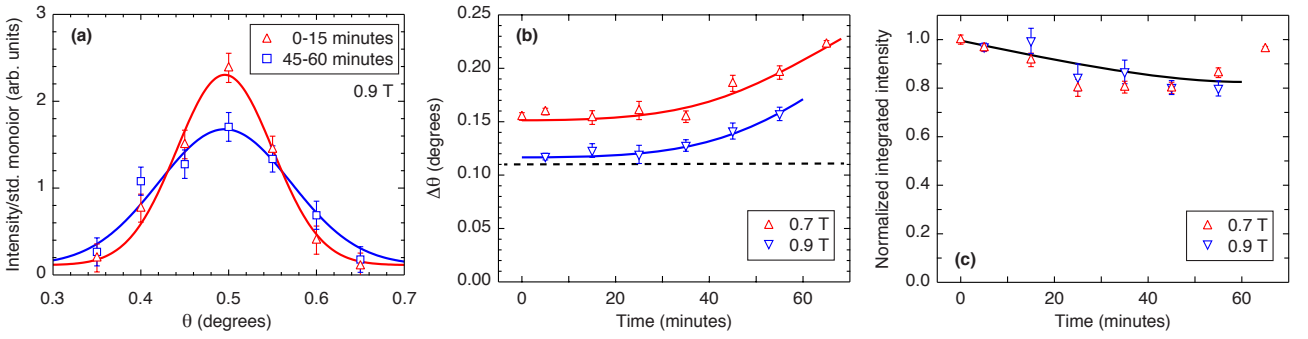


FIG. 3. (a) Rocking curves obtained on ZR8 at 0.9 T (ILL), measured during the first 15 minutes after the preparation of a pristine VL and after 45-60 minutes. Curves are Gaussian fits to the data as described in the text. (b) Time dependence of the fitted rocking curve width. The dotted line indicates the experimental resolution. (c) Time dependence of the fitted integrated intensity, normalized to the value for the pristine VL. Solid lines in (b) and (c) are guides to the eye.

was turned off. Again, the slight increase is likely due due to a lower sample temperature, and any re-ordering thus occurs on time scales much longer than the beam induced disordering if at all.

We now return to the broadening of the VL reflections perpendicular to the detector plane. Figure 3(a) shows rocking curves of the scattered intensity at 0.9 T as the split VL peak is rotated through the Bragg condition, where θ is the angle between the magnetic field and the neutron beam direction. An increase in the width and a reduction of the intensity at the rocking curve center ($\approx 0.5^\circ$) is clearly observed at the later time, consistent with Figs. 1 and 2 measured at the “rocked on” angle. The rocking curves are fitted to a Gaussian

$$I(\theta) = I_0 + \frac{I_{VL}}{\Delta\theta} \exp \left[-2 \ln(4) \left(\frac{\theta - \theta_0}{\Delta\theta} \right)^2 \right], \quad (1)$$

where I_0 is a constant offset, I_{VL} is proportional to the integrated intensity, θ_0 is the peak position and $\Delta\theta$ is the full width half maximum (FWHM). Values of I_0 and θ_0 were determined from the fit to the 0-15 minute data and then kept fixed. Fitted values of I_{VL} and $\Delta\theta$ as a function of time for fields of 0.7 T and 0.9 T are shown in Figs. 3(b) and 3(c) respectively. The integrated intensity is normalized to the value for the pristine VL, obtained either from measurements performed in the presence of a periodic ± 5 mT field oscillation (0.7 T) or by a linear extrapolation of I_{VL} to zero time (0.9 T).

The rocking curve width increases with time for both measured fields as seen in Fig. 3(b), confirming the gradual VL disordering hypothesized earlier. At all times $\Delta\theta$ for 0.9 T is less than for 0.7 T, indicating a more ordered VL at the higher field. This is consistent with our previous reports, measured in the presence of a periodic ± 5 mT field oscillation, of a VL ordering that increases with applied field up to 1.5 T [37]. At 0.9 T the $\Delta\theta$ approach the experimental resolution estimated by

$$\Delta\theta_{res.} = \sqrt{\delta\theta^2 + \left(\frac{q_{VL}\lambda_n}{2\pi} \frac{\Delta\lambda_n}{\lambda_n} \right)^2}, \quad (2)$$

where $\delta\theta$ is the standard deviation of the beam divergence, $\lambda_n = 0.75$ nm is the neutron wavelength, and $\Delta\lambda_n/\lambda_n = 15\%$ (ORNL) or 10% (ILL) is the FWHM wavelength spread [43]. Here $q_{VL} = 2\pi(2B/\sqrt{3}\phi_0)^{1/2}$ is the VL scattering vector and $\phi_0 = 2068$ T nm² is the flux quantum. The near constant value of $\Delta\theta$ during the first roughly 30 minutes indicates that the intrinsic width of the VL Bragg peaks is much smaller than $\Delta\theta_{res.}$, with a clear broadening observed only once the two becomes comparable. The inverse rocking curve width can thus be taken as a lower bound on the longitudinal VL correlation length, $\zeta_L \geq 2(q_{VL}\Delta\theta)^{-1} \approx 6 - 7 \mu\text{m}$. The absence of a time lag in reduction of the integrated intensity in Fig. 3(c) provides further evidence that the VL disordering begins as soon as the sample is subjected to the neutron beam. Here, I_{VL} decreases by $\sim 20\%$ within the first hour, possibly leveling off at the longer times (some recovery is suggested at 0.7 T but we hesitate to draw any conclusions based on a single data point). The decrease of the I_{VL} indicates a severe disruption of the VL, and possibly an evolution towards a vortex glass phase [42].

To quantify the VL disordering, measurements of the rocking curve peak intensity as a function of neutron exposure were performed for a range of magnetic fields. Figure 4(a) shows examples of decay curves for three different fields as a function of the total number of neutrons per area incident on the sample, demonstrating that the VL disorders more quickly at higher magnetic fields. The disordering rate is determined from simple linear fits, summarized in Fig. 4(b) for all measurement sequences and both UPt₃ crystals.

The fission events will locally heat the sample above the critical temperature, and perturb the vortices in the immediate vicinity. The persistence of a disordered vortex configuration after the thermal transient has dissipated is likely due to a quench through the vortex glass state which exists near the superconducting transition [5, 42], preventing the re-formation of an ordered VL. Support for such a scenario comes from SANS studies of NbSe₂, where the degree of VL ordering was found to depend sensitively on the thermal history in the vicinity of the so-called peak effect in

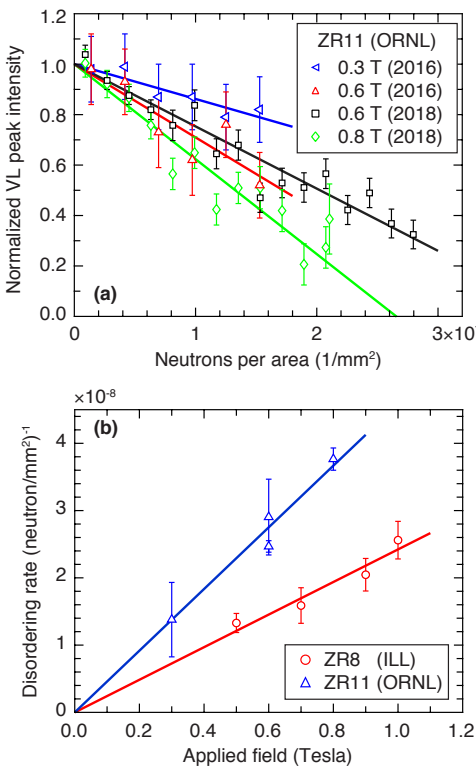


FIG. 4. (a) VL scattering rate vs neutrons per area transmitted through the sample for different fields. Data were obtained on ZR11 at ORNL during separate experiments (2016 and 2018). Intensities are normalized such that linear fits (solid lines) extrapolate to unity for the pristine VL. (b) Disordering rate vs magnetic field for both UPt₃ samples. Lines are linear fits to the ZR8 and ZR11 data, constrained to pass through the origin.

the critical current [15, 16, 44]. The peak effect is associated with the order-disorder transition between the vortex glass and Bragg glass states [45, 46], and is also observed in UPt₃ [47]. Furthermore, the ability to thermally quench the VL in UPt₃ was previously used to facilitate SANS studies of the superconducting A phase which exists just below T_c [17]. During roughly one month of accumulated irradiation ZR8 has experienced $\sim 10^{11}$ fission events (see Supplemental Material). This has not lead to a significant increase of the intrinsic vortex pinning as witnessed by the ability to achieve an ordered VL, indicating modest radiation damage to the UPt₃ crystals.

The volume affected by a single fission event may be estimated from the low-temperature specific heat ($C/T \approx 1.6T$ J/K³ mol) and the mass density ($\rho = 19.4$ g/cm³) of UPt₃ [48], yielding a sphere of diameter ~ 34 μ m heated above T_c . This should be considered as an order of magnitude estimate since it assumes the applicability of the equilibrium specific heat during the violent fission process and ignores both the field dependence of the specific heat [49] as well as the thermal conductivity [50]. With the vortex spacing given by $a_0 = (2\phi_0/\sqrt{3}B)^{1/2}$, the diameter obtained above corresponds to $\sim 400a_0 - 700a_0$ as the field is increased from 0.3 to 1 T. Therefore a single fission event does not only affect individual vortices

but a large section of the VL, with dimensions several times greater than the lower limit on the longitudinal correlation length obtained from the rocking curves.

A detailed understanding of the fission induced VL disordering will require a careful analysis, and is outside the scope of this Letter. In this regard, two important points may be deduced from Fig. 4(b). First, for each UPt₃ crystal the disordering rate is directly proportional to the applied magnetic field, indicating that it is governed by VL properties. Here, the elastic moduli, which increase with rising vortex density [6], will be important to consider as a greater stiffness will allow VL “shock waves” to propagate further from the volume directly affected by the fission events. Second, the ratio of the disordering rate to applied field differs for ZR8 and ZR11. The latter crystal is of higher quality (see Supplemental Material) and therefore expected to exhibit less vortex pinning. This will make the ZR11 VL less resilient against disordering, as disruptions can more easily propagate away from the fission volume. As stacking faults are the principal crystalline defects in UPt₃ [51] and directly visible in the small-angle background scattering [17], the relation between the disordering rate and sample quality should be quantified in future SANS experiments.

Before concluding we also consider how the fission events affect the superconducting order parameter in UPt₃ and our recent SANS experiments which provide direct evidence for broken time reversal symmetry in the B phase [37]. Here, differences in the VL orientation relative to the crystalline axes were observed between states with the Cooper pair orbital angular momentum either parallel or anti-parallel to the applied magnetic field. The latter corresponds to a metastable order parameter configuration, achieved by reducing the magnetic field at low temperature to enter the B phase and establish the chiral direction, eventually passing through zero and thus reverse the field direction. Fission events could potentially impact the chiral direction in the regions temporarily heated above T_c , and, if this direction is reversed upon re-cooling, lead to the formation of order parameter domain boundaries.

Based on the rate and affected volume, the fraction of the sample that remains unaffected by fission will decrease exponentially with a time constant of approximately 6 minutes. This is much shorter than the SANS count times which, at the higher fields, reach several hours. Since a difference in the VL was indeed observed between the two order parameter configurations [37], a fission induced reversal of the chiral direction, and the accompanying order parameter domain formation, does not appear to take place. This is consistent with both tunneling [52] and Kerr rotation [53] measurements, showing an absence of order parameter domain formation in UPt₃ even in the absence of a training field, and suggesting that a single order parameter domain spans the entire crystal [53]. Using the roughly 1 mm length scale associated with these experiments as a lower limit on the domain size yields a volume much greater than that affected by a fission

event. This implies that domain formation in UPt_3 is energetically unfavorable, and supports our conclusion that the order parameter in the SANS measurements is reformed with the same chiral direction as the surrounding sample.

In summary, we have shown that the VL in UPt_3 undergoes a gradual fission induced disordering when exposed to a beam of cold neutrons. Fission events heat regions of the sample above T_c which upon re-cooling hosts a quenched vortex glass state. The disordering rate is proportional to the vortex density, suggesting that it is governed by the VL stiffness. Our observations provide new possibilities for studies of vortex matter whereby local and reversible disorder can be combined with e.g. thermal disordering. We also speculate that the magnitude of field oscillation required for maintaining an ordered VL will be less than that needed to re-order a disordered VL due to the different structural properties. Finally, the use of periodic field oscillations to mitigate the VL disordering can be applied to other U-containing superconductors where SANS studies have to date been unsuccessful.

We are grateful to J. A. Sauls for numerous discussions over the years and to U. Köster for providing estimates of the sample heating due to fission. This work was supported by the U.S. Department of Energy, Office of Basic Energy Sciences, under Awards No. DE-SC0005051 (MRE: University of Notre Dame; neutron scattering) and DE-FG02-05ER46248 (WPH: Northwestern University; crystal growth and neutron scattering). A portion of this research used resources at the High Flux Isotope Reactor, a DOE Office of Science User Facility operated by the Oak Ridge National Laboratory. Part of this work is based on experiments performed at the Institut Laue-Langevin, Grenoble, France.

* Current address: Center for Exploration of Energy & Matter, Indiana University, Bloomington, Indiana 47408, USA

† Current address: Department of Physics and Astronomy, University of Kentucky, Lexington, Kentucky 40506, USA

‡ email: eskildsen@nd.edu

- [1] R. P. Huebener, *Magnetic Flux Structures in Superconductors* (Springer, 2001).
- [2] A. A. Abrikosov, Sov. Phys. JETP **5**, 1174 (1957).
- [3] W. H. Kleiner, S. H. Autler, and L. M. Roth, Phys. Rev. **133**, 1226 (1964).
- [4] J. Matricon, Phys. Lett. **9**, 289 (1964).
- [5] G. Blatter, M. V. Feigel'man, V. B. Geshkenbein, A. I. Larkin, and V. M. Vinokur, Rev. Mod. Phys. **66**, 1125 (1994).
- [6] E. H. Brandt, Rep. Prog. Phys. **58**, 1465 (1995).
- [7] T. Giamarchi and P. Le Doussal, Phys. Rev. B **52**, 1242 (1995).
- [8] T. Giamarchi and P. Le Doussal, Phys. Rev. B **55**, 6577 (1997).
- [9] T. Nattermann and S. Scheidl, Adv. Phys. **49**, 607 (2000).
- [10] P. Le Doussal, Int. J. Mod. Phys. B **24**, 3855 (2010).
- [11] M. Menghini, Y. Fasano, F. de la Cruz, S. S. Banerjee, Y. Myasoedov, E. Zeldov, C. J. van der Beek, M. Konczykowski, and T. Tamegai, Phys. Rev. Lett. **90**, 147001 (2003).
- [12] M. Checchin and A. Grassellino, Phys. Rev. Appl. **14**, 044018 (2020).
- [13] A. Romanenko, R. Pilipenko, S. Zorzetti, D. Frolov, M. Awida, S. Belomestnykh, S. Posen, and A. Grassellino, Phys. Rev. Appl. **13**, 034032 (2020).
- [14] Z. L. Xiao, O. Dogru, E. Y. Andrei, P. Shuk, and M. Greenblatt, Phys. Rev. Lett. **92**, 227004 (2004).
- [15] M. Marzali Bermudez, M. R. Eskildsen, M. Bartkowiak, G. Nagy, V. Bekeris, and G. Pasquini, Phys. Rev. Lett. **115**, 067001 (2015).
- [16] M. Marzali Bermudez, E. R. Louden, M. R. Eskildsen, C. D. Dewhurst, V. Bekeris, and G. Pasquini, Phys. Rev. B **95**, 104505 (2017).
- [17] A. Huxley, P. Rodière, D. M. Paul, N. van Dijk, R. Cubitt, and J. Flouquet, Nature **406**, 160 (2000).
- [18] P. Das, C. Rastovski, T. R. O'Brien, K. J. Schlesinger, C. D. Dewhurst, L. DeBeer-Schmitt, N. D. Zhigadlo, J. Karpinski, and M. R. Eskildsen, Phys. Rev. Lett. **108**, 167001 (2012).
- [19] S. Okuma, D. Shimamoto, and N. Kokubo, Phys. Rev. B **85**, 064508 (2012).
- [20] U. Yaron, P. L. Gammel, D. A. Huse, R. N. Kleiman, C. S. Oglesby, E. Bucher, B. Batlogg, D. J. Bishop, K. Mortensen, K. Clausen, C. A. Bolle, and F. de La Cruz, Phys. Rev. Lett. **73**, 2748 (1994).
- [21] U. Yaron, P. L. Gammel, D. A. Huse, R. N. Kleiman, C. S. Oglesby, E. Bucher, B. Batlogg, D. J. Bishop, K. Mortensen, and K. N. Clausen, Nature **376**, 753 (1995).
- [22] A. Duarte, E. Fernandez Righi, C. A. Bolle, F. de la Cruz, P. L. Gammel, C. S. Oglesby, E. Bucher, B. Batlogg, and D. J. Bishop, Phys. Rev. B **53**, 11336 (1996).
- [23] A. Pautrat, J. Scola, C. Simon, A. Brûlet, C. Goupil, M. J. Higgins, and S. Bhattacharya, Phys. Rev. B **71**, 064517 (2005).
- [24] G. Li, E. Y. Andrei, Z. L. Xiao, P. Shuk, and M. Greenblatt, Phys. Rev. Lett. **96**, 017009 (2006).
- [25] S. J. Levett, C. D. Dewhurst, and D. M. Paul, Phys. Rev. B **66**, 014515 (2002).
- [26] E. R. Louden, C. Rastovski, S. J. Kuhn, A. W. D. Leishman, L. DeBeer-Schmitt, C. D. Dewhurst, N. D. Zhigadlo, and M. R. Eskildsen, Phys. Rev. B **99**, 060502(R) (2019).
- [27] E. R. Louden, C. Rastovski, L. DeBeer-Schmitt, C. D. Dewhurst, N. D. Zhigadlo, and M. R. Eskildsen, Phys. Rev. B **99**, 144515 (2019).
- [28] M. R. Eskildsen, L. Y. Vinnikov, T. D. Blasius, I. S. Veshchunov, T. M. Artemova, J. M. Densmore, C. D. Dewhurst, N. Ni, A. Kreyssig, S. L. Bud'ko, P. C. Canfield, and A. I. Goldman, Phys. Rev. B **79**, 100501(R) (2009).
- [29] D. S. Inosov, T. Shapoval, V. Neu, U. Wolff, J. S. White, S. Haindl, J. T. Park, D. L. Sun, C. T. Lin, E. M. Forgan, M. S. Viazovska, J. H. Kim, M. Laver, K. Nenkov, O. Khvostikova, S. Kuhnemann, and V. Hinkov, Phys. Rev. B **81**, 014513 (2010).
- [30] D. S. Inosov, J. S. White, D. V. Evtushinsky, I. V. Morozov, A. Cameron, U. Stockert, V. B. Zabolotnyy, T. K. Kim, A. A. Kordyuk, S. V. Borisenko, E. M. Forgan, R. Klingeler, J. T. Park, S. Wurmehl, A. N. Vasiliev, G. Behr, C. D. Dewhurst, and V. Hinkov, Phys. Rev. Lett. **104**, 187001 (2010).
- [31] S. Mühlbauer, D. Honecker, E. A. Périgo, F. Bergner,

S. Disch, A. Heinemann, S. Erokhin, D. Berkov, C. Leighton, M. R. Eskildsen, and A. Michels, Rev. Mod. Phys **91**, 015004 (2019).

[32] W. T. Heller, M. Cuneo, L. Debeer-Schmitt, C. Do, L. He, L. Heroux, K. Littrell, S. V. Pingali, S. Qian, C. Stanley, V. S. Urban, B. Wu, and W. Bras, J. Appl. Crystallogr. **51**, 242 (2018).

[33] C. D. Dewhurst, J. Appl. Cryst. **47**, 1180 (2014).

[34] M. R. Eskildsen, K. Avers, C. Dewhurst, W. Gannon, W. P. Halperin, S. Kuhn, and J. White, “Chiral Effects on the Vortex Lattice in UPt_3 ,” Institut Laue-Langevin (ILL) doi:10.5291/ILL-DATA.5-42-402 (2016).

[35] M. R. Eskildsen, K. Avers, C. Dewhurst, D. Honecker, A. Leishman, and J. White, “Chiral Effects on the Vortex Lattice in UPt_3 ,” Institut Laue-Langevin (ILL) doi:10.5291/ILL-DATA.5-42-467 (2018).

[36] W. J. Gannon, W. P. Halperin, C. Rastovski, K. J. Schlesinger, J. Hlevyack, M. R. Eskildsen, A. B. Vorontsov, J. Gavilano, U. Gasser, and G. Nagy, New J. Phys. **17**, 023041 (2015).

[37] K. E. Avers, W. J. Gannon, S. J. Kuhn, W. P. Halperin, J. A. Sauls, L. DeBeer-Schmitt, C. D. Dewhurst, J. Gavilano, G. Nagy, U. Gasser, and M. R. Eskildsen, Nat. Phys. **16**, 531 (2020).

[38] R. Cubitt, E. M. Forgan, G. Yang, S. L. Lee, D. M. Paul, H. A. Mook, M. Yethiraj, P. H. Kes, T. W. Li, A. A. Menovsky, Z. Tarnawski, and K. Mortensen, Nature **365**, 407 (1993).

[39] T. Klein, I. Jounard, S. Blanchard, J. Marcus, R. Cubitt, T. Giamarchi, and P. Le Doussal, Nature **413**, 404 (2001).

[40] U. Divakar, A. J. Drew, S. L. Lee, R. Gilardi, J. Mesot, F. Y. Ogrin, D. Charalambous, E. M. Forgan, G. I. Menon, N. Momono, M. Oda, C. D. Dewhurst, and C. Baines, Phys. Rev. Lett. **92**, 237004 (2004).

[41] M. Laver, E. M. Forgan, A. B. Abrahamsen, C. Bowell, T. Geue, and R. Cubitt, Phys. Rev. Lett. **100**, 107001 (2008).

[42] R. Toft-Petersen, A. B. Abrahamsen, S. Balog, L. Porcar, and M. Laver, Nat. Commun. **9**, 901 (2018).

[43] J. S. Pedersen, D. Posselt, and K. Mortensen, J. Appl. Crystallogr. **23**, 321 (1990).

[44] N. D. Daniilidis, S. R. Park, I. K. Dimitrov, J. W. Lynn, and X. S. Ling, Phys. Rev. Lett. **99**, 147007 (2007).

[45] P. L. Gammel, U. Yaron, A. P. Ramirez, D. J. Bishop, A. M. Chang, R. Ruel, L. N. Pfeiffer, E. Bucher, G. D’Anna, D. A. Huse, K. Mortensen, M. R. Eskildsen, and P. H. Kes, Phys. Rev. Lett. **80**, 833 (1998).

[46] I. Jounard, J. Marcus, T. Klein, and R. Cubitt, Phys. Rev. Lett. **82**, 4930 (1999).

[47] U. Yaron, P. L. Gammel, G. S. Boebinger, G. Aeppli, P. Schiffer, E. Bucher, D. J. Bishop, C. Broholm, and K. Mortensen, Phys. Rev. Lett. **78**, 3185 (1997).

[48] R. Joynt and L. Taillefer, Rev. Mod. Phys. **74**, 235 (2002).

[49] A. P. Ramirez, N. Stücheli, and E. Bucher, Phys. Rev. Lett. **74**, 1218 (1995).

[50] H. Suderow, J. P. Brison, A. Huxley, and J. Flouquet, J. Low Temp. Phys. **108**, 11 (1997).

[51] J.-I. Hong, *Structure-Property Relationships for a Heavy Fermion Superconductor UPt_3* , Ph.D. thesis, Northwestern University (1999).

[52] J. D. Strand, D. J. Van Harlingen, J. B. Kycia, and W. P. Halperin, Phys. Rev. Lett. **103**, 197002 (2009).

[53] E. R. Schemm, W. J. Gannon, C. M. Wishne, W. P. Halperin, and A. Kapitulnik, Science **345**, 190 (2014).

SUPPLEMENTAL MATERIAL

UPt₃ Single Crystals

Both ZR8 and ZR11 are long, rod-like crystals and were cut into two pieces which were co-aligned and fixed with silver epoxy (EPOTEK E4110) to a copper cold finger for the SANS measurements. For each SANS experiment the respective sample assembly was mounted onto the mixing chamber of a dilution refrigerator and placed inside a superconducting magnet, oriented with the crystalline **a** axis vertical and the **c** axis horizontally along the magnetic field and the neutron beam. For both samples the neutron beam was masked off to illuminate a 7×11 mm² area.

Sample properties of the two UPt₃ single crystals are listed in Table I. These are determined from resistive measurements performed on small samples cut from the main crystals. Here, RRR is the residual resistivity ratio, T_c is the superconducting transition temperature and ΔT_c is the width of the transition. The greater RRR and smaller ΔT_c for ZR11 indicates its higher quality compared with ZR8.

Sample	mass (g)	RRR	T_c (mK)	ΔT_c (mK)
ZR8	15	> 600	560 ± 2	10
ZR11	9	> 900	557 ± 2	5

TABLE I. Properties of the two UPt₃ single crystals used for the SANS experiments.

Fission event rate

A determination of the fission event rate is difficult to achieve directly from the SANS measurements since the neutron beam attenuation is dominated by non-fissile absorption by ²³⁸U and Pt. It may, however, be estimated from the fissile heating of the sample, where an incident flux of 1.1×10^6 neutrons/second was found to cause a ~ 1.3 μ W reduction of the heating power required to maintain the dilution refrigerator mixing chamber at a constant temperature. This greatly exceeds the kinetic energy/second of the incident neutrons of 0.2 fW. Assuming a net energy release of 200 MeV, the observed heating yields 4×10^4 fission events per second. Adjusting for the sample transmission ($\approx 60\%$ for ZR8) this corresponds to roughly 6% of the incident neutrons, and a ²³⁵U concentration of $\sim 0.3\%$ which is typical for depleted uranium. The ZR8 and ZR11 crystals were grown from the same batch of uranium, and are therefore expected to have the same concentration of ²³⁵U. The different disordering rates between the two samples in Fig. 4(b) is therefore not due to different fission rates.